Magnetic assembled nanostructures from pure and mixed Co-based clusters

2004 J. Phys.: Condens. Matter 16 S2231

(http://iopscience.iop.org/0953-8984/16/22/024)

INSTITUTE OF PHYSICS PUBLISHING JOURNAL OF PHYSICS: CONDENSED MATTER

J. Phys.: Condens. Matter **16** (2004) S2231–S2240 PII: S0953-8984(04)74480-X

Magnetic assembled nanostructures from pure and mixed Co-based clusters

V Dupuis, L Favre, S Stanescu, J Tuaillon-Combes, E Bernstein and A Perez

Laboratoire de Physique de la Matière Condensée et Nanostructures, Université Claude Bernard Lyon I and CNRS, 69622 Villeurbanne Cédex, France

E-mail: Veronique.Dupuis@lpmcn.univ-lyon1.fr

Received 6 October 2003
Published 21 May 2004
Online at stacks.iop.org/JPhysCM/16/S2231
DOI: 10.1088/0953-8984/16/22/024

Abstract

The low energy cluster beam deposition (LECBD) technique is used to prepare original magnetic nanostructures from Co-based clusters preformed in the gas phase and subsequently embedded in non-magnetic matrices in ultrahigh vacuum. Nanostructured films of pure cobalt and mixed CoM clusters (with M = Ag or Pt) with controlled sizes and compositions have been investigated. We study the correlations between the specific structure, morphology and the resulting magnetic properties obtained for individual nanoclusters by the highly sensitive microSQUID magnetometry technique and on assemblies of non-interacting clusters by conventional techniques. From the role of various contributions, we will underline at the nanometre scale the dominant role of the surface/interface effects on the magnetic anisotropy.

1. Introduction

The preparation of original magnetic nanostructures and the study of their specific properties are playing an increasingly important role due to the large number of potential applications in various fields such as information storage and magnetoelectronic devices (Sun *et al* 2000, Sellmyer *et al* 1999). The magnetic behaviour of individual isolated nanoscale systems has mainly been theoretically approached while experimental investigations are limited by the sensitivity of magnetic characterization techniques. In bulk magnetic materials (3D), volume magnetocrystalline energies are the main sources of anisotropy whereas in lower dimensionality systems such as thin films (2D), wires (1D) or clusters (0D), strong surface effects are expected. Consequently, the necessity to provide quantitative information on the different contributions to the magnetic anisotropy is of particular importance for future applications of such small systems (Sun *et al* 2000). At present, the use of one single cluster as the ultimate information storage bit is forbidden at room temperature because of its superparamagnetic behaviour (i.e. spontaneous magnetization reversal as a result of thermal

fluctuation effects). To attempt to overcome this limitation, we developed novel magnetic Co-based clusters with a rather high anisotropy in order to remain magnetically oriented up to room temperature or above. Mixed CoM clusters (with M = Ag and Pt) were prepared from a laser vaporization source by the low energy cluster beam deposition (LECBD) technique. After deposition in ultrahigh vacuum, their structural and magnetic behaviours are studied as a function of the embedding matrix nature (Nb and MgO) and compared to the properties of the pure Co clusters embedded in Pt, Ag, Nb and MgO matrices.

2. Experimental procedures

Cluster assembled films are prepared by deposition of low energy clusters preformed in the gas phase (Perez *et al* 1997). For that purpose, a cluster generator based on a combined laser vaporization–gas condensation source has been developed to produce intense supersonic jets of nanoclusters with sizes ranging from a few tens to a few thousands of atoms (diameter from one to a few nanometres). Briefly, a YAG laser ($\lambda = 532$ nm, pulse duration of a few nanoseconds, frequency up to 30 Hz) is used to vaporize a mixed CoM target rod mounted in the source chamber. A continuous flow of inert gas (He or a mixture He + Ar, from 20 up to 60 mbar) is injected into the source chamber to cool the plasma generated at the target surface and to nucleate clusters which are subsequently completely stabilized in the supersonic expansion taking place at the exit nozzle of the source. It has been previously verified that bimetallic clusters produced from this source roughly exhibit the same composition as the compound target one (PtPd (Rousset *et al* 1995), AuNi (Rousset *et al* 2000), AuAg (Gaudry *et al* 2001)). However, depending on some specific effects such as segregation, atoms can be non-homogeneously distributed in the cluster. Neutral clusters can be deposited, without fragmentation in the LECBD regime, on various substrates to grow nanogranular films in ultrahigh vacuum (UHV) conditions. Moreover, by co-depositing on a 45°-tilted substrate in the UHV-deposition chamber an atomic beam emitted from an e-beam evaporator, it is possible to produce films of clusters embedded in various matrices (metallic, oxides). Since both cluster and atomic beams are independent, this last technique allows the production of any kind of cluster/matrix system, even with miscible elements, in a wide range of cluster concentrations.

High resolution transmission electron microscopy (HRTEM) observations are performed *ex situ* to characterize the atomic structure of isolated supported clusters and cluster assembled nanostructures. In this case, deposits below the 2D-percolation threshold (coverage rate lower than 50%) on amorphous carbon coated grids, are performed and subsequently protected by a thin silicon layer on top before removal in air. Structural characterizations on collections of clusters by x-ray techniques (diffraction and absorption (Tuaillon *et al* 1997, Dupuis *et al* 2003a, 2003b) using the synchrotron radiation facilities at LURE—Orsay, France) are performed with a view to confirming that the structure is conserved for clusters embedded in any matrix and to precisely define the local Co atoms' environment in both mixed and embedded clusters. Magnetic nanostructures from pure or mixed cobalt clusters are studied using various complementary techniques in order to investigate the magnetic behaviour from an isolated individual cluster to an assembly of non-interacting clusters. For that purpose, the ultrahigh sensitivity magnetometry technique based on microSQUID devices developed to detect the magnetic signal of one single nanoparticle with sizes as low as 1000 atoms (Jamet *et al* 2001a, 2001b) is used by embedding the Co-based clusters directly in the niobium film constituting the superconducting loop at temperatures lower than 7 K. For magnetic measurements on cluster assemblies, the conventional SQUID magnetometry technique is used, complemented by x-ray magnetic circular dichroism (XMCD) measurements (Jamet *et al* 2000) in the case of a superconducting matrix to probe the magnetism of clusters at a local scale.

Table 1. Experimental coordination numbers of Co in two sites: $N_{\mathrm{Co-Co}}$ and $N_{\mathrm{Co-M}}$ (with M = Ag, Pt or Nb) as deduced from the fits of the EXAFS spectra.

Simulated EXAFS spectra	$N_{\mathrm{Co-Co}}$	$N_{\mathrm{Co-M}}$
Co/Ag	11	1
Co/Pt	9.6	2.4
Co/Nb	7	5

3. Experimental results and discussion

3.1. Pure cobalt clusters

From TEM observations, supported Co clusters deposited without any matrix present a log-normal size distribution with a mean diameter D around 3–4 nm. High resolution observations allowed us to conclude that Co clusters exhibit a truncated octahedron morphology with a fcc-structure. From anomalous x-ray diffraction experiments we verified that Co clusters keep at least a fcc-core even when they were embedded in a miscible matrix. For a fine study of the local environment of Co atoms in a grain, we performed x-ray absorption experiments using the synchrotron radiation source at the Co K edge (7713 eV) on Co/Ag, Co/Pt and Co/Nb samples with cluster concentrations lower than the 3d percolation threshold. By only considering the first neighbours in the Fourier transform of the extended x-ray absorption fine structures (EXAFS) signal and by using the FEFFIT code, we distinguished Co-atoms in the core of the grains with a bulk-like structure, Co-atoms with a high Debye–Waller coefficient σ (a few hundredth of ångströms which corresponds to metal–metal dilated distances) and finally the Co–M environment (Dupuis *et al* 2003a). Corresponding coordination numbers ($N_{\mathrm{Co-Co}}$ and $N_{\mathrm{Co-M}}$) reported in table 1 are given with a precision of ± 1.

To interpret these results, we calculated the coordination numbers using a core-shell model based on a pure cobalt core and a mixed interface (with 50% of Co and 50% of M) for a number of diffuse surface layers varying from 0 to 2. Then we compared these theoretical coordination numbers to the experimental ones obtained for the Co/Ag, Co/Pt and Co/Nb samples (table 1). The ideal non-miscible Co/Ag couple led to the sharpest interface with no diffuse surface layer (sites with a theoretical coordination number $N_{\mathrm{Co-M}}$ equal to 1.4). The miscible Co/Pt couple can be approximated by a diffuse interface limited to one-monolayer (sites with a theoretical coordination number $N_{\mathrm{Co-M}}$ equal to 3.2). And finally, we obtained two diffuse layers at the interface in the Co/Nb miscible couple (sites with a theoretical coordination number $N_{\mathrm{Co-M}}$ up to 5).

Field-cooled (FC) and zero-field cooled magnetization measurements on Co/M samples were performed using conventional magnetometry techniques. In diluted samples, with volume cluster concentrations below 15%, we observed a typical superparamagnetic behaviour. The blocking temperature T_{B} can be defined as the temperature where the relaxation time $\tau = \tau_0 \exp(\Delta E / k_{\mathrm{B}} T)$ is equal to the measuring time τ_{mes}. ΔE corresponds to the anisotropy energy barrier to be crossed in order to reverse the particle magnetization. In our case, τ_{mes} is of the order of a few second and the attempt frequency τ_0^{-1} is typically 10^9–10^{12} Hz. In figure 1, we report the blocking temperature T_{B} estimated from the maximum of the ZFC curves at 10 mT applied magnetic field. For comparison, one can mention that the lowest blocking temperature ($T_{\mathrm{B}} \sim 12$ K) is obtained for the Co/Nb sample, whereas the greatest one ($T_{\mathrm{B}} \sim 87$ K) is obtained for the Co/Pt sample, both being composed by miscible couples. For two non-miscible couples, namely Co/Ag and Co/SiO_2 samples, we measured similar $T_{\mathrm{B}} \sim 30$ K (Parent *et al* 1997). The magnetic diameter D_{m} of the nanoparticles determined

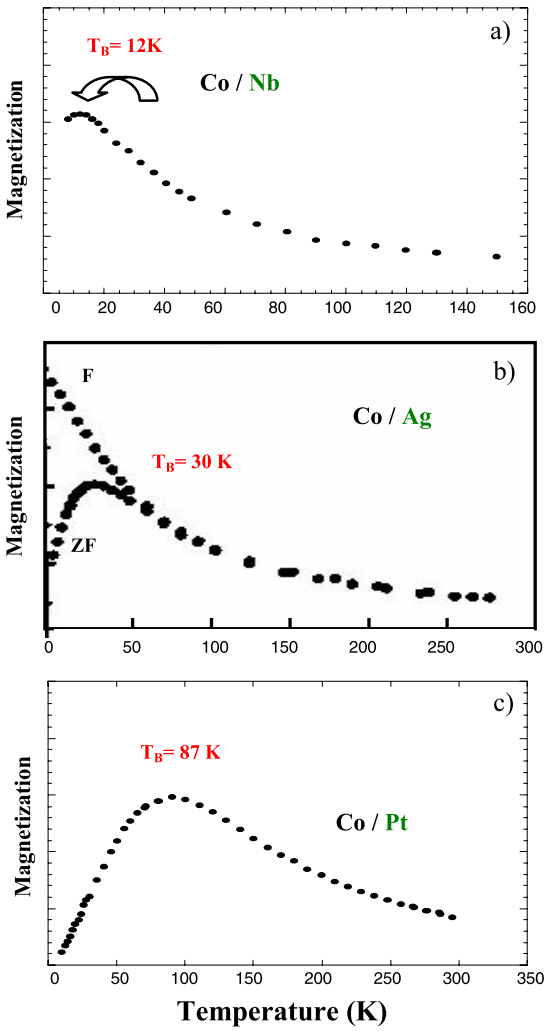

Figure 1. FC and ZFC magnetization curves obtained for films of Co clusters embedded (a) in a Nb-matrix, (b) in an Ag-matrix and (c) in a Pt-matrix. Measurements were performed with a 10 mT applied magnetic field.

(This figure is in colour only in the electronic version)

from a Curie–Weiss susceptibility law in the superparamagnetic state above T_B, was found to be the same for both samples and roughly equal to the size determined from TEM observations of Co clusters. By contrast, for the Co/Nb sample we found a reduced 'magnetic size' with respect to the TEM one (Jamet *et al* 2001b). So, we can conclude that the Co/Nb alloyed interface probably acts as a 'magnetically dead layer'. In the case of the Co/Pt system, to explain the large T_B value observed in agreement with the proposed core-shell model, we should consider an increase of magnetization at the interface (Jamet *et al* 2001a). Finally, for all Co/M samples we found that the cluster saturation magnetization can be written in the form:

$$M_s(T) = xM_s^{\text{core}}(T) + (1-x)M_s^{\text{shell}}(T).$$

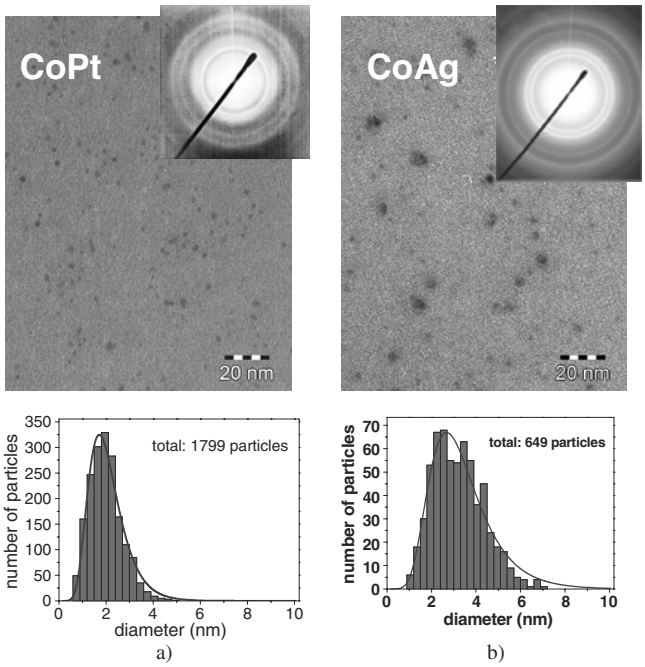

Figure 2. Size distribution of deposited CoPt (a) and CoAg (b) clusters derived from TEM observations. The solid curve represents the best fit of the size distribution obtained using a log-normal function to deduce the mean cluster diameter $D = 2$ nm (a) and $D = 3$ nm (b).

According to previous EXAFS results, one atomic layer is expected to be mixed at the interface for the Co/Pt sample, giving $x = 0.63$. By assuming that $M_s^{core}(T) = M_s^{bulk}(T)$, a magnetization at the interface $M_s^{shell}(0) = 1900$ kA m^{-1} is obtained (to compare with $M_s^{core}(0) = 1430$ kA m^{-1}). In the Co/Nb case, $M_s^{shell}(0)$ is taken to be equal to zero and $x = 0.36$, because of the presence of two 'magnetically dead' alloyed monolayers at the cluster–matrix interface, leading to the very low experimental value of $M_s(0) = 515$ kA m^{-1}. Finally, for non-miscible couples such as Co/Ag, the sharp interface roughly induces $x = 1$ and a bulk-like magnetization value for the corresponding sample. In the particular case of Co/Nb samples, because the superconducting fluctuations in the niobium matrix below its critical temperature (T_c(Nb) $= 7$ K) prevent any conventional magnetization measurements at low temperature, we used additional XMCD experiments as a local and selective magnetometry technique in the low temperature range. From hysteresis loops measured in the temperature range 5–50 K for all the samples, we deduced the remanent magnetization and the corresponding effective anisotropy constant K_{eff} related to ΔE as follows: $\Delta E = K_{eff} D_m^{\alpha}$, where $\alpha = 2$ means a surface anisotropy and $\alpha = 3$ a volume one. Finally, in a first approximation, the anisotropy energy of the system can be seen as a sum of both volume and surface contributions leading to the following equation:

$$K_{eff} D_m^{\alpha} = K_V V + K_S S. \tag{1}$$

The values of all these parameters for the Co/Pt and Co/Nb systems are reported in table 2.

Concerning the Co/Nb samples with $\alpha = 2.5$, the origin of the effective anisotropy is not clear, while the surface anisotropy clearly dominates for the Co/Pt ones. For this last case, we can notice that such results have already been observed for Co/Pt multilayers with high perpendicular anisotropy (Hillebrands and Dutcher 1993, Lin *et al* 1991) and

Table 2. Values of the exponent α in equation (1), volume-anisotropy constant K_V and surface-anisotropy constant K_S obtained for Co/Pt and Co/Nb samples.

Sample	α	K_V (10^5 J m^{-3})	K_S (10^{-4} J m^{-2})
Co/Pt	2	—	3
Co/Nb	2.5	0.5	5

have been attributed to high spin–orbit coupling effects in such systems. To go further, we decided to determine the origin of K_{eff} in individual nanoparticles directly embedded in the niobium superconducting loop of the microSQUID device (Jamet *et al* 2001b). The experimental anisotropy measured for our individual Co clusters is probably related to an interface anisotropy resulting from the symmetry breaking at the cluster surface and the presence of additional facets on the perfect polyhedron (Jamet *et al* 2003). Nevertheless, it is clear that the superparamagnetic limit prevents the use at room temperature of pure cobalt particles with sizes lower than 10 nm in high density storage media.

3.2. Bimetallic cobalt-based clusters

3.2.1. CoAg mixed clusters. We previously showed that the direct contact between the magnetic Co-nanoparticles and the superconducting Nb-matrix leads to a magnetically dead layer at the cluster surface. To avoid such an effect, we prepared new systems consisting of mixed CoAg clusters where a segregation of silver atoms at the cluster surface is expected (Rousset *et al* 2000). From a thermodynamical point of view, the lower surface energy of silver compared to the cobalt one (γ(Ag) = 1250 mJ m^{-2} and γ(Co) = 2550 mJ m^{-2}), its higher atomic radius (r(Ag) = 1.13 Å and r(Co) = 0.74 Å) and the immiscible character of the Co–Ag couple, are in favour of silver surface segregation. From *ex situ* TEM observations, deposited CoAg clusters exhibit a log-normal size distribution with a mean diameter of about 3 nm (∼1200 atoms) and a standard deviation $\sigma = 0.40$ (see figure 2). Complementary Rutherford backscattering analysis (RBS measurements with 2 MeV α-particles) on 80 nm thick-films of Co–Ag clusters, protected by a thin silicon layer on top, were performed to determine the mean compositions of the supported cluster-assemblies. Using a $Co_{0.5}Ag_{0.5}$ target, we obtained mixed Co–Ag clusters with a mean atomic composition of 57% Co and 43% Ag (±2%). The crystallographic structure was first investigated by electron diffraction on a thick (30 nm) Co–Ag cluster film. Figure 2 clearly shows that both silver and cobalt are crystallized in their own fcc-structures which seems to indicate that segregation occurs. To determine the atomic composition of individual clusters we performed energy dispersive x-ray (EDX) experiments on a few hundred separated particles with a Jeol 2010 F scanning TEM (STEM) and a high EDX resolution (probe size of about 5 nm) allowing measurements on single clusters (Holderer *et al* 2003). A rather broad composition dispersion is revealed with an average value of the cobalt atomic concentration of about 58% in agreement with RBS results. In table 3 we give the number of surface atoms as a function of the cluster size in the case of perfect truncated octahedrons. So by assuming a complete silver-atom surface segregation, one can underline that the Ag concentration is a critical parameter for the smallest clusters.

As an indirect way of probing whether the core-shell morphology is obtained or not, we embedded the Co–Ag clusters in an MgO-matrix to study the possible Co–O neighbouring. From XPS and EXAFS measurements performed on CoAg/MgO samples, an important oxide (CoO-type) contribution has been evidenced, leading to irreversible damage of the magnetic properties of the CoAg samples. In particular, a paramagnetic behaviour has been observed on CoAg/MgO samples from SQUID magnetometry experiments related to a transition from

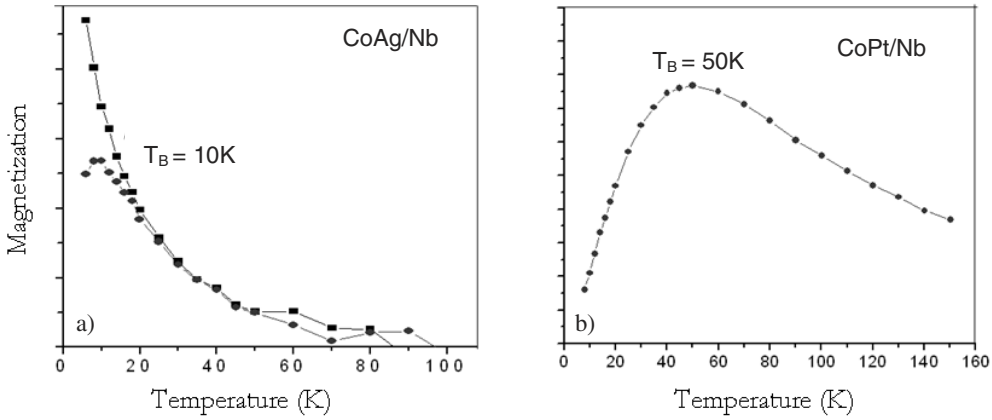

Figure 3. FC and ZFC magnetization curves obtained for films of CoAg (a) and CoPt (b) mixed clusters embedded in a Nb-matrix. Measurements were performed with a 10 mT applied magnetic field.

Table 3. Number of atoms located at the cluster surface calculated for a series of perfect fcc-truncated octahedrons.

Number of atoms per cluster ⇒ mean diameter	1 surface ML (% of atoms)	2 surface ML (%)
201 atoms ⇒ 1.6 nm	60.7	90.5
586 atoms ⇒ 2.4 nm	46.4	79.1
1289 atoms ⇒ 3.3 nm	37.4	64.4
2406 atoms ⇒ 4 nm	31.3	55.5

the high spin to the low spin state as in Co/MgO samples. Moreover, for mixed CoAg/Nb samples, we obtained magnetic characteristics identical to those of Co/Nb samples (with a TEM diameter of 4 nm for cobalt clusters, i.e. ∼2400 atoms /cluster): T_B around 10 K and a coercive field of a few hundred Oersted (see figure 3). By taking into account that only 35% of Co atoms are magnetic in pure Co/Nb samples (because of the two magnetically dead layers at the interface (Jamet *et al* 2001a, 2001b)), and that 50–60% are cobalt atoms in CoAg clusters, we obtain an equivalent number of 600–700 magnetic atoms in both systems. This could explain the similar magnetic characteristic of both Co/Nb and CoAg/Nb samples, if we assume an equivalent anisotropy. Nevertheless, it is not the case if we compare the microSQUID measurements on individual clusters, where fouth order anisotropy energy terms due to magnetocrystalline anisotropy contribution appear in the CoAg/Nb samples whereas second order terms dominated in Co/Nb ones (Jamet *et al* 2003). If we assume that Ag atoms segregate at the surface of mixed clusters, preventing direct contact between the magnetic clusters and the surrounding matrix for the larger clusters, a new Co/Ag/Nb interface has to be considered instead of the Co/Nb one. In that case, the compensation of the shape and surface anisotropy terms at the Co/Ag interface induces the second order surface terms vanishing in aid of the fourth order one. (Dupuis *et al* 2003b).

3.2.2. CoPt mixed clusters. We decided to study CoPt samples because, in this case, a hybridization effect between the 3d Co and the 5d Pt orbitals is expected, leading to high magnetization and magnetic anisotropy increases as previously mentioned in Co/Pt samples.

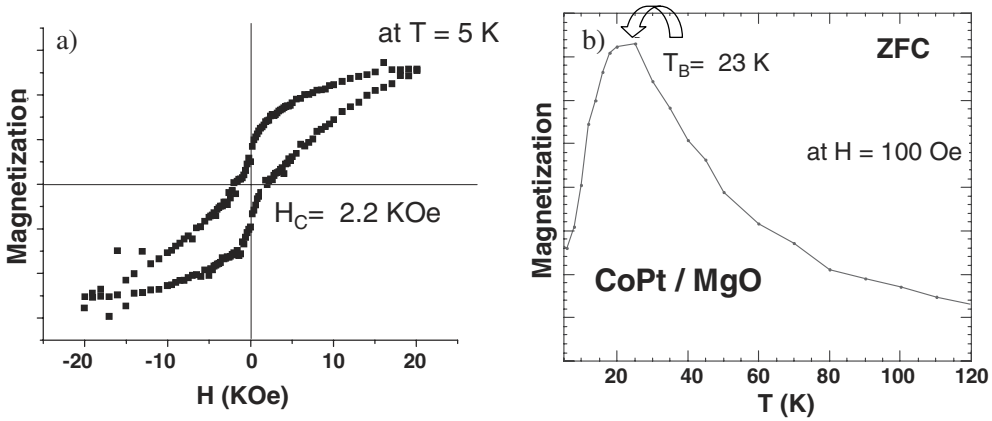

Figure 4. Hysteresis loop measurements at 5 K (a) and ZFC magnetization curves (b) obtained on CoPt mixed clusters embedded in the MgO matrix.

The main interest in CoPt magnetic nanoparticles is to understand the factors controlling their magnetic anisotropy energy (MAE). In our previous experimental results on nanosize samples, we systematically underlined the importance of the cluster/matrix interface effects. Recently, Felix-Medina *et al* (2003) theoretically studied the ground state spin moments (m_s), orbital moments (m_l) and MAE of CoPd clusters in the framework of the self-consistent tight-binding method. They demonstrated that it is the interface composition rather than just the reduction of the local coordination number at the surface which is responsible for the enhancement of orbital moments and of MAE in magnetic clusters. Calculations on CoPt clusters are in progress.

As in the case of CoAg mixed samples, the use of a nanosecond pulsed laser and a continuous inert gas flow in the cluster source have been found necessary to conserve the CoPt target stoichiometry. From TEM observations on deposited clusters, only one phase is observed and identified as a fcc CoPt phase. The nanocrystallites size distribution has been found centred around 2 nm in diameter (see figure 2). GISAXS (grazing incidence small angle x-rays scattering) measurements at LURE-Orsay, show that the CoPt clusters conserved a 2 nm size when embedded in a matrix.

SQUID magnetometry measurements performed on CoPt/Nb samples reveal an increase of the blocking temperature T_B up to 50 K. This T_B value is intermediate between 12 K obtained for Co/Nb samples and 87 K for Co/Pt ones whereas the number of cobalt atoms in a mixed CoPt-cluster is about 300 compared to one thousand for pure Co-cluster. At this stage, a T_B increase being related to an enhancement of the energy barrier ΔE and ($\Delta E = K_{\text{eff}} D_{\text{m}}^{\alpha}$), we need to improve both K_{eff} and D_{m} contributions (i.e. the number of magnetic atoms) in the same way to increase T_B up to room temperature for applications to high density storage media. The coercive field H_c in CoPt/Nb samples also increased up to 750 Oe at low temperature. Hybridization effects between Co and Pt are probably at the origin of a magnetic moment induced in the platinum and of the MAE increase because of the presence of a strong spin–orbit coupling. When CoPt clusters are embedded in MgO, T_B is equal to 23 K and H_c to 2200 Oe (see figure 4). Once more, to explain such variations, interactions between the clusters and the oxide matrix are to be considered in terms of magnetocrystalline or more probably in terms of exchange anisotropy (antiparallel coupling between a ferromagnetic core and an antiferromagnetic shell), which avoids an easy line-up of magnetic moments along the applied magnetic field (Parasote *et al* 1999, Berkowitz *et al* 1999).

Magnetometry measurements as a function of temperature are in progress, as well as XMCD on mixed Co_xPt_{1-x} cluster samples in order to investigate the effect of Pt atoms on the bimetallic nanoparticles compared to multilayers samples (Grange *et al* 2000).

4. Conclusion

Well-defined structural and magnetic properties at every scale are absolutely necessary to unambiguously determine the anisotropy terms involved in bimetallic nanoclusters. In particular, element-selective techniques using synchrotron radiation seem promising to reveal the role of all species in the magnetic properties of complex, mixed and diluted systems. By comparing the magnetic properties of three kinds of Co-based clusters (Co, CoAg and CoPt) embedded in various matrices, we have underlined the dominant role of the surface/interface effects on the magnetic anisotropy because of the rivalry between the number of core and surface atoms. The structural morphology of mixed clusters sharply related to surface segregation effects has also been found of great importance to understand the magnetization reversal under an applied magnetic field. Finally, we clearly showed that, depending on the cluster/matrix nature, interface interactions could lead to antagonist effects from improvement of magnetic properties (as in Co/Pt) up to a paramagnetic behaviour (as in Co/MgO). A good compromise between many parameters (as cluster composition, size, magnetic moment, anisotropy and compatibility with the matrix) has to be found before we are be able to use an ordered network of clusters as storage media.

Acknowledgments

The authors are indebted to O Boisron, G Guiraud and C Clavier for their continuous and efficient technical assistance during the cluster preparations and LECBD experiments. The authors would like to thank A Traverse and O Lyon from LURE in Orsay, France, and D Babonneau from the University of Poitiers, for their assistance during the absorption and diffraction experiments using the synchrotron radiation sources. Many thanks also to the research group of W Wernsdorfer and B Barbara from the Laboratoire Louis Neel in Grenoble, France for their assistance during magnetic measurements performed on their installations.

We gratefully acknowledge support from the EC (AMMARE contract No G5RD-CT 2001-0047P) for some parts of the work reported in this paper.

References

Berkowitz A E *et al* 1999 *J. Magn. Magn. Mater.* **200** 552

Dupuis V, Favre L, Jamet M, Tuaillon-Combes J, Melinon P and Perez A 2003a *J. Vac. Sci. Technol.* A **21** 1519

Dupuis V, Favre L, Stanescu S, Tuaillon-Combes J, Bernstein E and Perez A 2003b Review of 'recent research developments in magnetism and magnetic materials' *Transworld Res. Netw.* **1** 101

Felix-Medina R *et al* 2003 *Phys. Rev.* B **67** 094430

Gaudry M, Lerme J, Cottancin E, Pellarin M, Prevel B, Treilleux M, Melinon P, Rousset J L and Broyer M 2001 *Eur. Phys. J.* D **16** 201

Grange W *et al* 2000 *Phys. Rev.* B **62** 1157

Hillebrands B and Dutcher J R 1993 *Phys. Rev.* B **47** 6126

Holderer O, Epicier T, Esnouf C and Fuchs G J 2003 *Phys. Chem.* B **107** 1723

Jamet M, Dupuis V, Melinon P, Guiraud G, Perez A, Wernsdorfer W, Traverse A and Baguenard B 2000 *Phys. Rev.* B **62** 493

Jamet M, Negrier M, Dupuis V, Tuaillon-Combes J, Melinon P, Perez A, Wernsdorfer W, Barbara B, Vogel J and Baguenard B 2001a *J. Magn. Magn. Mater.* **237** 293

Jamet M, Wernsdorfer W, Thirion C, Dupuis V, Mailly D, Melinon P and Perez A 2001b *Phys. Rev. Lett.* **86** 4676

Jamet M, Wernsdorfer W, Thirion C, Dupuis V, Melinon P, Perez A and Mailly D 2004 *Phys. Rev.* B **69** 024401
Lin C J *et al* 1991 *J. Magn. Magn. Mater.* **93** 194
Parasote V *et al* 1999 *J. Magn. Magn. Mater.* **198/199** 375
Parent F, Tuaillon J, Dupuis V, Prevel B, Perez A, Melinon P, Guiraud G, Steren L B, Morel R, Barthelemy A and Fert A 1997 *Phys. Rev.* B **55** 3683
Perez A, Melinon P, Dupuis V, Jensen P, Prevel B, Tuaillon J, Bardotti L, Martet C, Treilleux M, Broyer M, Pellarin M, Vialle J L, Palpant B and Lerme J 1997 *J. Phys. D: Appl. Phys.* **30** 709
Rousset J L, Cadette Santos Aires F J, Sekhar B R, Melinon P, Prevel B and Pellarin M 2000 *J. Phys. Chem.* B **104** 5430
Rousset J L, Cadrot A M, Cadette Santos Aires F J, Renouprez A, Melinon P, Perez A, Pellarin M, Vialle J L and Broyer M 1995 *J. Chem. Phys.* **102** 8574
Sellmyer D J, Yu M and Kirby R D 1999 *Nanostruct. Mater.* **12** 1021
Sun S, Murray C B, Weller D, Folks L and Moser A 2000 *Science* **287** 1989
Tuaillon J, Dupuis V, Melinon P, Prevel B, Treilleux M, Perez A, Pellarin M, Vialle J L and Broyer M 1997 *Phil. Mag.* A **76** 493